6

Finite Element Analysis in Orthopaedic Biomechanics

Daniel Kluess, Jan Wieding, Robert Souffrant,
Wolfram Mittelmeier and Rainer Bader
University of Rostock, Department of Orthopaedics
Rostock, Germany

1. Introduction

Based on the evolution of today's personal computers and workstations, numerical simulation gained an important significance in biomechanical research. A common tool in numerical simulation is the finite element method (FEM), which can be applied in various ways, e.g. in structure mechanics, thermodynamics or acoustics. The field of orthopaedic biomechanics utilises two major numerical approaches: musculo-skeletal research is based on multi-body-dynamics, dealing with kinematics of the skeletal systems and muscle activity. The second, structure-mechanical point-of-view deals with stress and strain analysis of bone, joints (natural and artificial) and load-bearing implants. Finite-element-analysis (FEA) is the preferred method for this second group of numerical problems occurring in orthopaedic biomechanics.

Due to the resolution of the calculated mechanical parameters, e.g. stress and strain, the results get more accurate the more elements the analysed structure is divided into. Taking a closer look at literature reveals how the development of faster and also affordable computers accelerated the finer mesh density of FE-models over the past years. A FE-model of the pelvis, published in 1995 by Dalstra et al. (Dalstra, Huiskes et al. 1995) and frequently cited, consisted of 2,602 elements. Five years later, Garcia et al. (Garcia, Doblare et al. 2000) reported results gained from a FE-model of the pelvis consisting of 6,425 elements. In 2006, in conjunction with the development of higher-performance workstations, Manley et al. (Manley, Ong et al. 2006) presented their pelvis model using almost 300,000 finite elements.

However, even the finest mesh density and accuracy of results is useless if the orthopaedic researchers fail to draw clinical relevance out of their analyses. Naturally, despite very few exceptions, the FE analysts are engineers, who need to make their results understandable to a clinician not familiar with numerical simulation.

What is the key to a fruitful communication between engineers and clinicians? What enlivens the circle between clinical input and provision of analytical results? At first, both the clinician and the engineer have to get used to the other one's subject-specific language. Each should be familiar with fundamental terms in order to enable a successful communication. Further, the clinician needs to know the potentials of numerical analysis. It

unquestionably is beneficial if the clinician can also question the engineer's results, which necessitates the clinician's basic understanding of the pitfalls in numerical analysis.
On the other hand, the engineer needs the clinician's input in terms of e.g. boundary conditions, geometry and material. By following these guidelines, a curriculum of the 'input of relevant clinical questions' and 'provision of solutions with analytical background', as depicted in Fig. 1, can be achieved.

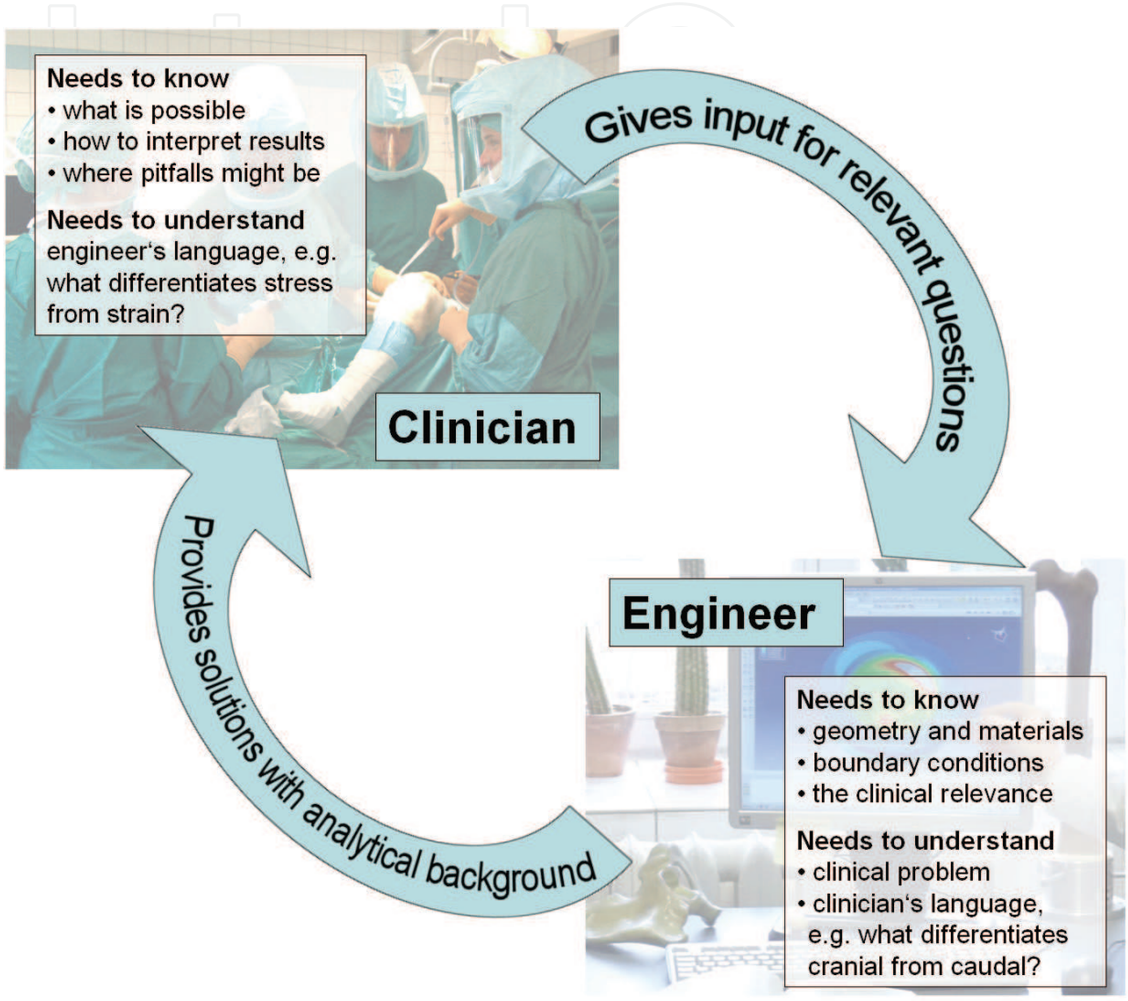

Fig. 1. Communication and knowledge scheme in numerical orthopaedic biomechanics between clinician and engineer

In orthopaedic biomechanics, as well as in related areas of expertise, such as traumatology research or dental biomechanics, modelling of the problem necessitates consideration of bone, implants and both combined, called the implant-bone-compound. As it is the most common implant in orthopaedic surgery, we want to take a closer look at the total hip replacement (THR).
There are about 500,000 THR surgeries in Europe (150,000 in Germany) each year (Aldinger, Jung et al. 2005), with growing numbers throughout the world. Implantation of an artificial hip joint has become a standard procedure in the past decades and the enhanced

performance of today's implants draws attention to younger and more active patients. The major indication for THR is arthrosis, a degenerative disease of the hip joint, which is caused by destruction of the hip joint cartilage.
The modern THR consists of the acetabular component and the femoral component (Fig. 2). The acetabular component usually is a metal shell which holds an insert, mainly made of polyethylene or ceramics. The metal shell is either impacted (press-fit) or screwed (threaded) in the prepared acetabulum. The femoral component consists of the stem and the ball-head. The prosthetic head can be made of either ceramics or cobalt-chromium. The prosthetic stem is, in the majority of THR, made of titanium alloy (Ti-6Al-4V). The mainly used bearings are ceramic-on-ceramic, ceramic-on-polyethylene and metal-on-polyethylene.
Despite the good results achieved with THR, there is still a number of serious complications that require further research on implant design, implant material, bearing material, coating and many more.

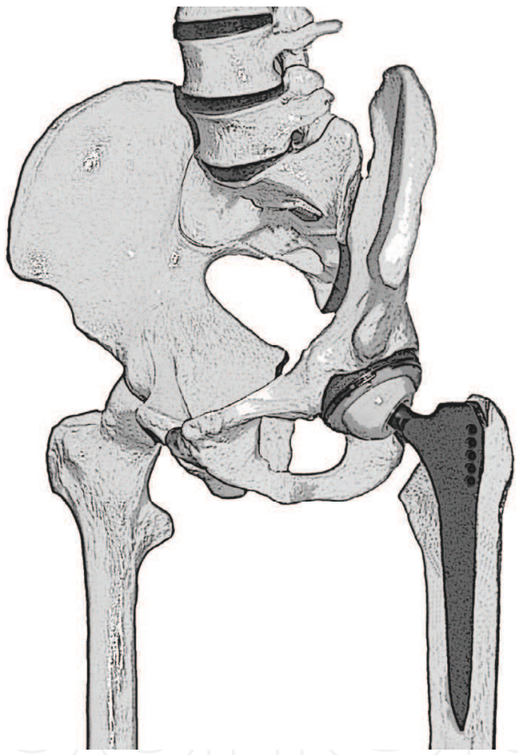

Fig. 2. Total hip replacement (THR) displayed in the surrounding bone with cut view of the proximal femur

The finite-element-method is used frequently in implant development, helping to answer unresolved questions related to clinical complications. Presently, various approaches to generate models of the implant-bone-compound in THR are published (Spears, Pfleiderer et al. 2001; Thompson, Northmore-Ball et al. 2002; Kaku, Tsumura et al. 2004; Oki, Ando et al. 2004; Manley, Ong et al. 2006). However, these models each have its issues in being reproducible by the reader. In any case, these issues occur because it was not the publisher's focus to describe the methodology in detail, but to present their results.

In the following chapter of this paper, we firstly want to present a convenient modus operandi of generating FE-models of the implant-bone-compound which can be reproduced by other scientists. We developed an approach starting from computed tomograms of the patient and corresponding CAD-models of the implant. The algorithm is aimed at predicting the stress and strain states in the surrounding bone stock and in the implant itself and has the potential to predict relative micromotion.
Furthermore, we show an example of how this modelling approach can be applied. Therefore, a finite-element study of a newly developed implant for acetabular cup revision (exchange of the acetabular component after implant loosening) is demonstrated.

2. How to generate finite-element-models of the implant-bone-compound

Opposed to other scientific displicines in engineering and design, the analyzed structures in Orthopaedic Biomechanics are not man-made, but of biological origin. Hence, when bone is analyzed, there are no exactly defined angles, curves and distances, but patient-specific morphology which is highly inhomogeneous and which changes over lifetime, depending on physiological loads, health, age and nutrition. Bone morphology is mainly determined by genetic factors, but also by mechanics, as discovered by the German orthopaedic surgeon Julius Wolff (Wolff 1892). Wolff's law states that bone has the ability to adapt to mechanical loads, i.e. the external and internal structure of bone is transformed depending on the load occuring in the bone. Especially with regard to implant technology and arthroplasty, bone transformation plays an important role. If the biomechanical distribution of forces in and around the treated joint is reconstructed inappropriately during surgery, or if the design of the implant is improper, so-called 'stress shielding' can occur. If the forces are mainly transferred by the implant, adjacent bony regions get minimally loaded and are subsequently degraded. This is another problem that can be solved by stress and strain analysis of the implant-bone-compound.
Modern imaging methods like computed tomography (CT) and magnetic resonance tomography (MRT) allow reconstruction of biological structures for computational finite-element-analysis, whereby CT is the method of choice for bone. The three-dimensional reconstruction is the basis for the presented approach.
On the other hand, the implants to be analyzed in the finite-element-model can be designed using CAD-software, imported from the manufacturer's data or can also be three-dimensionally reconstructed from scan data, e.g. laser-scanning point clouds.
Starting from CT-data of bone and CAD-data of the implant, our approach to model the implant-bone-compound is demonstrated in Fig. 3. A stepwise description of the single modules follows.
The algorithm is based on a number of software packages used (Table 1). The mentioned software modules are not mandatory; however, during development of this algorithm, we found no relevant issues in interfaces and data transfer using these packages.
In the following subchapters, a detailed description of the single steps included in the algorithm is given.

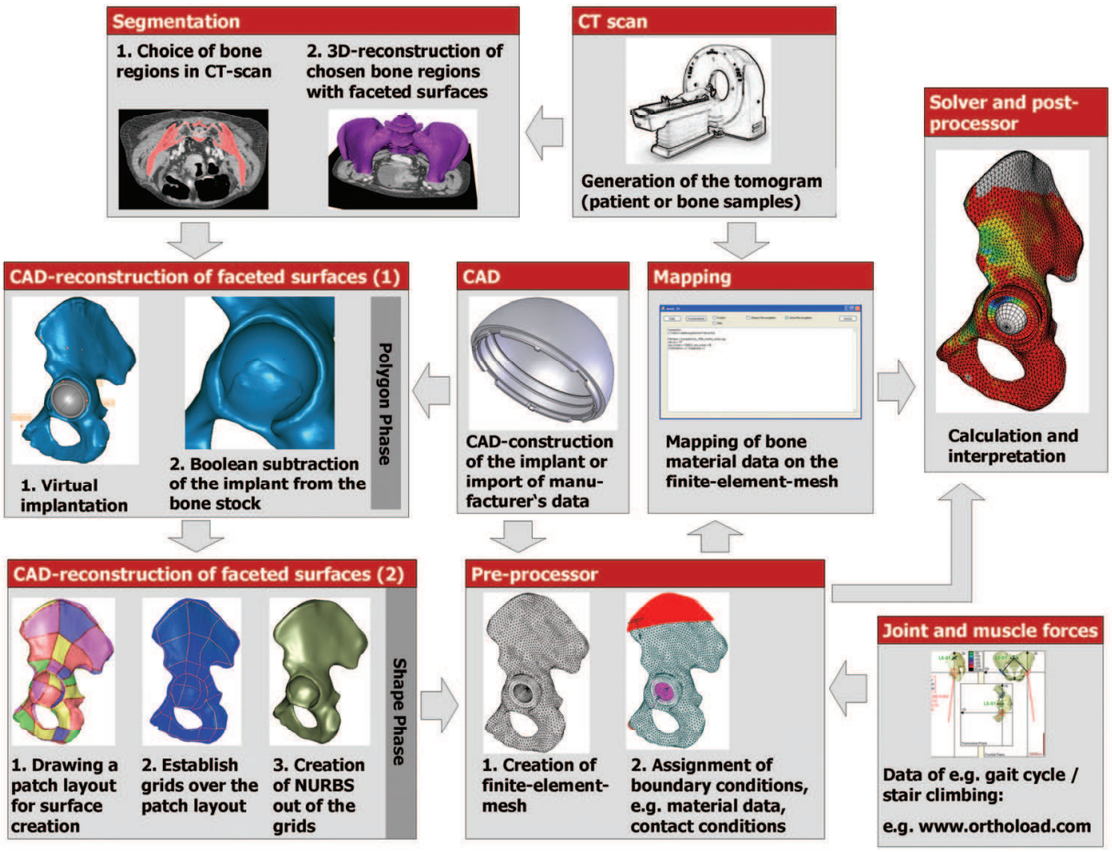

Fig. 3. Approach to analyze the implant-bone-compound via finite-element-methods

Purpose	Software	Manufacturer / Distributor
Segmentation	AMIRA	Mercury Computer Systems Inc., MA, USA
CAD-reconstruction of faceted surfaces	GEOMAGIC STUDIO	Raindrop Geomagic, NC, USA
CAD	SOLIDWORKS	Dassault Systèmes, RI, USA
Mapping	AMAB	Self-developed program, University of Rostock, Germany
Pre-processor	MSC/PATRAN	Marc Schwendler Corp., CA, USA
Solver	Simulia/ABAQUS	Dassault Systèmes, RI, USA
Post-processor	Simulia/ABAQUS Viewer	Dassault Systèmes, RI, USA

Table 1. Software used for generating the presented finite-element-models (not mandatory, other software packages, e.g. CAD-software, are considered equivalent)

2.1 Three-dimensional reconstruction of bone morphology

The reconstruction of bone morphology is based on a stack of CT-slices showing the designated bone. In our approach, we make use of the correlation of bone stiffness and attenuation (Snyder and Schneider 1991; Rho, Hobatho et al. 1995). The level of attenuation is measured in Hounsfield Units (HU), which are typically used in the DICOM-files of the CT-scans. HU are normalized in the way that air has a value of -1,000 and water has a value of 0. Bone usually has HU of 250-3,000. The DICOM-files which include all of the sectional slices calculated by the CT scanner are imported into the software AMIRA. After the bony structures are labeled in all slices of the CT-scans, an automatic three-dimensional reconstruction of the bone is performed creating triangulated surfaces (Fig. 4).

2.2 Virtual implantation and CAD-transformation of faceted surfaces

After the bone is imported in the software GEOMAGIC, the virtual implantation can be undertaken. It might be necessary to adjust the position of the bone in order to achieve a definite implant position There are recommendations for placing coordinate systems at bones and joints given by the International Society of Biomechanics (Wu, Siegler et al. 2002; Baker 2003; Wu, van der Helm et al. 2005). At this point it is very important to record the 4*4 transformation matrix, so the adjustment can be undone at a later stage using the inverse of the transformation matrix..

When the bone is adjusted properly, the CAD-file of the implant can be imported in GEOMAGIC using the IGES interface. The bone stock can be prepared for virtual implantation by subtracting the implant geometry from the bone morphology. Additionally, press-fit cavities can be created by downscaling the implant before subtraction. Since the bone is existent in GEOMAGIC's polygon phase, the implant also has to be transformed to a polygon model before the Boolean subtraction is performed. Implant placement plays a major role in order to generate an adequate model of the implant-bone-compound. In clinical application, implant placement is determined via the surgery manual, the instruments (e.g. cutting guide) as well as accurately defined angles. For example, the acetabular cup in total hip replacement is placed according to lateral abduction, also known as inclination, as well as anteversion. Nevertheless, an orthopaedic surgeon should be consulted in order to verify an adequate virtual implantation.

After the cavity is created in the bone, the next important step is to convert the faceted polygon surfaces to analytical non-uniform rational b-spline surfaces (NURBS). NURBS are analytically defined surfaces which are based on control points. The calculation and definition of NURBS is a major advantage compared to discrete tessellated surfaces. On the one hand, this allows a better performance of CAD modelling, on the other hand, the analytical surfaces can be distributed such that an automatic hexahedral meshing operation can be facilitated (Fig. 5).

When the faceted surfaces are converted into NURBS properly, the bone can be transferred to a pre-processor using the IGES interface. Provided the surfaces form a waterproof body, PATRAN is able to convert these surfaces to one solid. Then the solid can be meshed automatically with tetrahedral finite elements.

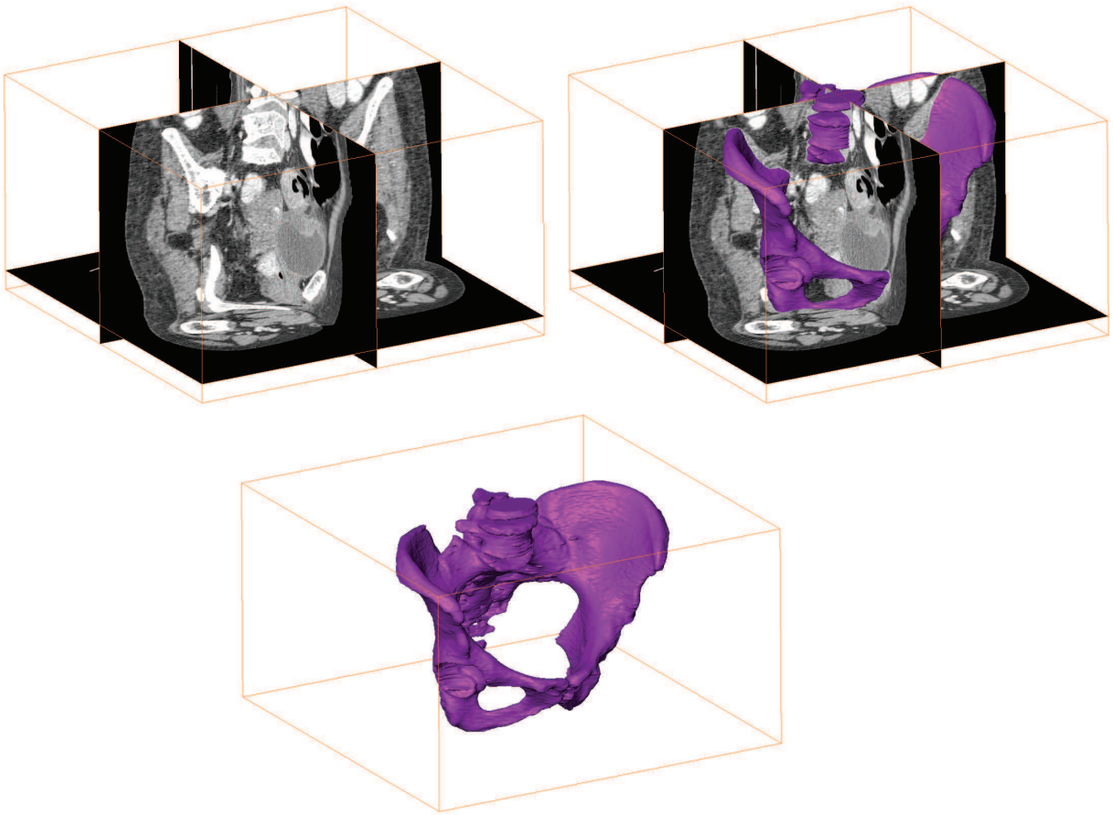

Fig. 4. Three-dimensional reconstruction of bone from CT-scan data using AMIRA. Bone morphology is exported as a tesselated surface.

Fig. 5. Distribution of NURBS-surfaces such that quadrilateral surfaces are oppositely located enables generation of solids with five or six faces. Such solids can be meshed with hexahedral elements automatically.

2.3 Mapping of material data on the finite-element-mesh

Mapping of material data from the CT slices onto the finite-element-mesh is a common procedure in finite-element-analysis nowadays (Thompson, Northmore-Ball et al. 2002;

Anderson, Peters et al. 2005; Manley, Ong et al. 2006; Schultze, Kluess et al. 2007). The most common technique is to map the HUs onto the elements and to assign a high number of different material definitions corresponding to equivalent ranges of HU. However, our approach is to handle the HU as temperatures and to assign a temperature-dependent material model (Zacharias 2001; Schultze, Kluess et al. 2007). Hence, the mapping is not proceeded element-wise, but node-wise. Instead of defining several material models for the different ranges of HU, only one material definition depending on the assigned temperatures is needed, resulting in a cost-effective and time-saving calculation. This also enables consideration of cortical bone with a constant Young's modulus as well as consideration of trabecular bone with a HU-dependent modulus using the same temperature-dependent material definition.

There are both material models for trabecular bone which depend directly on the HU (Snyder and Schneider 1991; Rho, Hobatho et al. 1995) and material models which depend on the apparent density respectively the Calcium equivalence (Snyder and Schneider 1991; Dalstra, Huiskes et al. 1993; Keller 1994). To correlate the HU from the CT scans with apparent density and Calcium equivalence, a bone mineral density phantom must be CT-scanned together with the relevant bone.

Using a Toshiba tomograph (Aquilion 32, TOSHIBA Medical Systems GmbH, Germany) at 120 kV and 300 mAs, we found a linear correlation between HU and Calcium density (Fig. 6).

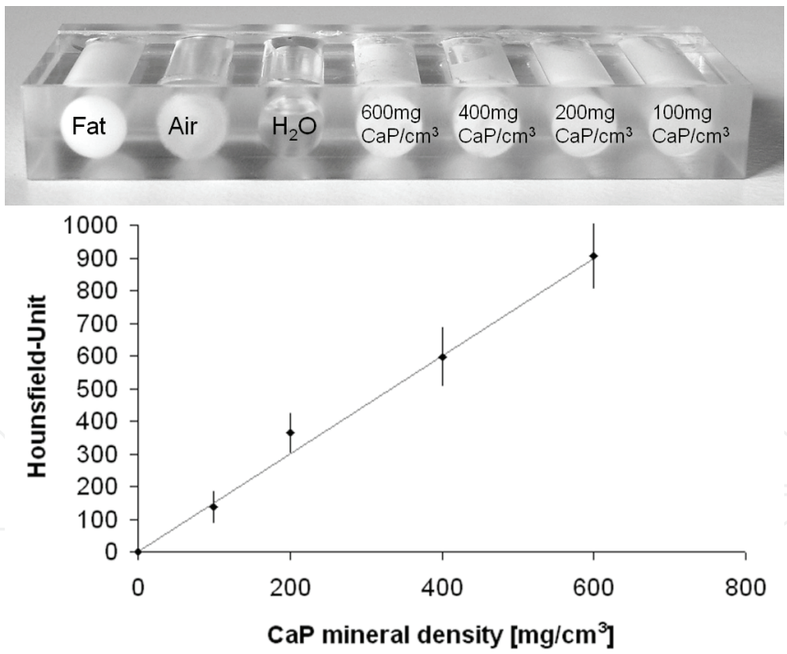

Fig. 6. Top: Custom made bone mineral density phantom. Bottom: Correlation between HU and Calcium mineral density determined by using the bone mineral density phantom.

With our custom-made mapping algorithm (AMAB, University of Rostock), each nodal coordinate of the FE-mesh is retrieved in the stack of CT-slices by detecting firstly the coronal height (axis z) and secondly the location in the coronal plane (axis x and y). The HU

in the corresponding location in the CT slices are averaged within a definite zone surrounding the nodal coordinates. The software allows adjustment of the averaging zone by means of height and width. A weighting algorithm is included which increases the weight of the HU in closer proximity to the FE-node's location during averaging. Besides the density distribution in cancellous bone, the varying thickness of pelvic cortical bone can be represented with high accuracy.

2.4 Applying boundary conditions

The application of boundary conditions in biomechanical FEA is based on assumptions including forces and pressures acting in the human body, as well as displacements and symmetry boundary conditions based on simplifications in the model. The major source of acting loads in the musculoskeletal system for orthopaedic biomechanics is the telemetric in-vivo measurement using instrumented implants (Bergmann, Graichen et al. 1993; Bergmann, Deuretzbacher et al. 2001; D'Lima, Patil et al. 2006). Some of the data gathered by Bergmann et al. is now available online at http://www.orthoload.com.

Furthermore, the calculation of acting muscle forces by means of inverse dynamics as a numerical approach yields growing potential in musculoskeletal biomechanics (Rasmussen, Damsgaard et al. 2003). Future steps in musculoskeletal biomechanics will have as their goal the implementation of inverse dynamics with regard to kinematics into finite-element-methods in a combined model.

3. Application of the finite-element-method for preclinical analysis of an endoprosthetic implant

Following the presentation of how to generate finite-element-models of the implant-bone-compound, an example of the application of this algorithm is given. Therefore, we take a closer look at the clinical problem first.

3.1 Clinical background and objective

Despite the technical advances in THR the number of revisions (exchange of a failed implant) in the United States doubled from 1990 till 2002 (Kurtz, Mowat et al. 2005). The major indication for revision of approx. 75 % of failed THR is aseptic loosening (Malchau, Herberts et al. 2002). The reasons why, in turn, revisions fail are instability (35%) and again, aseptic loosening (30%) (Springer, Fehring et al. 2009). The occurrence of failed THRs displaying massive deficiencies in acetabular bone stock is enhanced by the increasing number of total hip arthroplasties.

Numerous implant systems with different fixation principles, specially designed for acetabular cup revision, have been developed so far and have revealed fair to good clinical results. The cemented systems include acetabular roof rings (Siebenrock, Trochsler et al. 2001; Gerber, Pisan et al. 2003; Yoon, Rowe et al. 2003) and antiprotrusio cages (Peters, Curtain et al. 1995; Wachtl, Jung et al. 2000; Perka and Ludwig 2001; Weise and Winter 2003; Gallo, Rozkydal et al. 2006), which are usually implanted in combination with autografts. Cementless acetabular revision systems include bilobed components (DeBoer and Christie 1998; Chen, Engh et al. 2000), oval shaped cups (Götze, Sippel et al. 2003; Haury, Raeder et al. 2004; Civinini, Capone et al. 2007), pedestal cups (Perka, Schneider et al. 2002; Schoellner

2004) and oversized acetabular components (Dearborn and Harris 2000; Whaley, Berry et al. 2001). Most of the non-cemented acetabular revision systems are designed for a small range of defects and do not provide the modularity necessary to adapt to the wide range of patient-individual bone morphology and defect sizes seen at reoperation.
The presented example of a finite-element-study in Orthopaedic Biomechanics forms the basis in the development of a new acetabular cup revision system capable of providing a cementless solution. The development is aimed at patient individual situations for enhanced fixation of the cup by additional polyaxial and angular stable fixation pegs as well as a modular adaptable lateral flap. The body of the revision cup is oblong shaped to fit the acetabular defect without sacrificing too much bone in the anterior and posterior column. The lateral flap is available in different angles to fit the patient's pelvic morphology individually. An outstanding feature of the fixation pegs is the ability to apply the pegs right after the cup is impacted into the bone. Consequently, the orthopaedic surgeon can decide whether to use one, two or no fixation pegs based on the objective primary stability established by press-fit of the cup and the optional additional fixation using the flap. Moreover, the fixation pegs provide angular stable fixation with the cup within a rotation angle of 16°.
The objective using the finite-element-method is to predict the biomechanical performance of the new implant system in terms of micromotion and stress states in the bone. The biomechanical analysis is carried out by modeling different combinations of fixation pegs and the lateral flap used with the implanted revision cup system and applying loads corresponding to the gait cycle and stair climbing. The calculated micromotion in the implant-bone-compound gives a prediction of how the primary stability of the newly developed acetabular cup revision system can be enhanced using additional fixation.

3.2 Methods

The CAD prototype of the newly developed acetabular cup revision system is shown in Fig. 7. The lateral flap is attached using a dove-tail in combination with two securing screws and locking rings. The implant system contains three different flaps with ascending blade angles to account for the patient-individual pelvic morphology. The flaps are anatomically shaped to provide optimum fit onto the underlying bone. Each lateral flap is manufactured with three drill holes for the application of bone screws.
In order to analyze the biomechanical performance of the additional fixation elements, a FE-model of the pelvis with the implanted revision cup system was modelled using our methodology from the previous chapter. Peak loads from walking and from stair climbing were applied. The morphology of a hemi-pelvis was reconstructed from high resolution computed-tomography (CT) (slice distance 0.3 mm). The hemi-pelvis was oriented in a Cartesian coordinate system, with the x-axis connecting the right and left spinae iliacae anterior superior (SIAS), the y-axis touching the pubic symphysis and pointing cranially and the z-axis pointing anteriorly.
An acetabular bone defect of D'Antonio Type III (D'Antonio, Capello et al. 1989) was created in the computer model of the hemi-pelvis. Afterwards, the osteolysis-modified bone structure was imported into the software GEOMAGIC (Raindrop Geomagic, NC, USA) for virtual implantation of the revision system. For that purpose, the CAD-model of the revision cup system was oriented at the pelvic coordinate system and placed in 45° lateral abduction and 20° anteversion.

Fig. 7. CAD-prototype of the newly developed acetabular cup revision system with modular adaptable lateral flap and fixation pegs

Subsequently, the acetabular bone stock was prepared by Boolean subtraction of the implant volume from the pelvic volume. The hemi-pelvis was meshed with 10-node tetrahedral finite elements, the acetabular revision system as well as the liner were meshed with 8-node hexahedral finite elements and the prosthetic head was modeled as an analytical rigid surface (Preprocessor: Patran, MSC, CA, USA). A stick-slip contact formulation with a friction coefficient of μ = 0.6 was assigned between implant and bone. The assembled FE-mesh is shown in Fig. 8. Constraints were applied at the sacroiliac joint (fully constrained) and the pubic symphysis (symmetry boundary conditions).

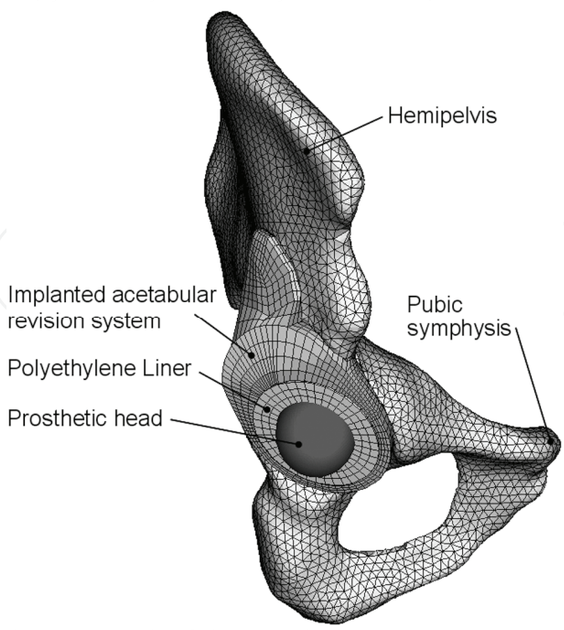

Fig. 8. Assembled finite-element-mesh of the acetabular cup revision system and the surrounding bone. Instead of meshing, the prosthetic head was modeled as an analytical rigid surface.

The material model of the bone was based upon the bone mineral distribution derived from the CT-scans. Our custom-made bone mineral density phantom was CT-scanned together with the analyzed pelvis. The Hounsfield Units (HU) in 100 voxels of each of these chambers in the CT scans were measured in order to gain the analytical relationship between the attenuation, measured in HU, and the bone mineral density, measured in Calcium-Equivalence ($\rho_{Ca\text{-}Eq}$):

$$HU = 1{,}4997\,\rho_{Ca-Eq} \tag{1}$$

Using equation (1), the material model for pelvic trabecular bone from Dalstra et al.(Dalstra, Huiskes et al. 1993) could be applied. Calcium-Equivalence $\rho_{Ca\text{-}Eq}$ was converted to Apparent Density ρ_{app}:

$$\rho_{app} = \frac{\rho_{Ca-eq}}{0{,}626} \tag{2}$$

This conversion is followed by the correlation of Young's modulus of trabecular bone E_{trab} and Apparent Density ρ_{app} (Dalstra, Huiskes et al. 1993):

$$E_{trab} = 2017{,}3\,\rho_{app}^{2{,}46} \tag{3}$$

In the FE-model, Apparent Density ρ_{app} was mapped from the CT scans onto each node and treated mathematically as temperatures. Using a temperature-dependent material model, the distribution of stiffness in trabecular and subchondral bone was calculated as a function of Apparent Density ρ_{app} respectively Calcium-Equivalence $\rho_{Ca\text{-}Eq}$. Areas with $\rho_{Ca\text{-}Eq} > 700$ were assigned a constant Young's modulus of E_{cort} = 8.5 GPa and treated as cortical bone (Kluess, Souffrant et al. 2009).

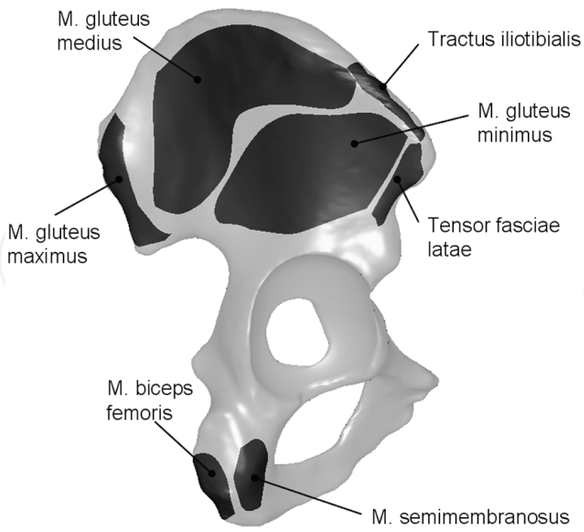

Fig. 9. Attachment areas of simulated muscle forces in the FE-model acting at the hip joint.

The muscle forces acting at the hip joint as well as the hip force resultant during normal gait and during stair climbing were extracted from telemetric measurements (Bergmann, Graichen et al.

1993; Bergmann, Deuretzbacher et al. 2001) and corresponding calculations (Heller, Bergmann et al. 2001). The acting muscles were concentrated into separate groups according to Fig. 9.
The amounts of the distributed force vectors in the FE-model are summarized in Tab. 2, given in percentage of the patient's bodyweight (80.0 kg respectively 748.4 N). The hip force resultant was applied in the reference node of the analytical rigid surface located in the center of the reconstructed hip joint.

Muscles	Normal gait			Stair climbing		
	F_x (%BW)	F_y (%BW)	F_z (%BW)	F_x (%BW)	F_y (%BW)	F_z (%BW)
Abductors (Mm. glutei maximus, medius, minimus)	-58.0	-86.5	-4.3	-70.1	-84.9	-28.8
M. biceps femoris	-0.6	-4.1	0.5	-	-	-
Tensor fasciae latae	-7.2	-13.2	-11.6	-3.1	-2.9	-4.9
M. semimembranosus	-17.6	-57.4	-0.8	-	-	-
Tractus iliotibialis	-	-	-	-10.5	-12.8	3
Hip force resultant F_R	54	229.2	-32.8	59.3	236.3	-60.6

Table 2. Applied muscle forces and hip force resultant during normal gait and during stair climbing. The amounts are given in percentage of the patient's bodyweight (%BW) (Bergmann, Graichen et al. 1993; Bergmann, Deuretzbacher et al. 2001; Heller, Bergmann et al. 2001)

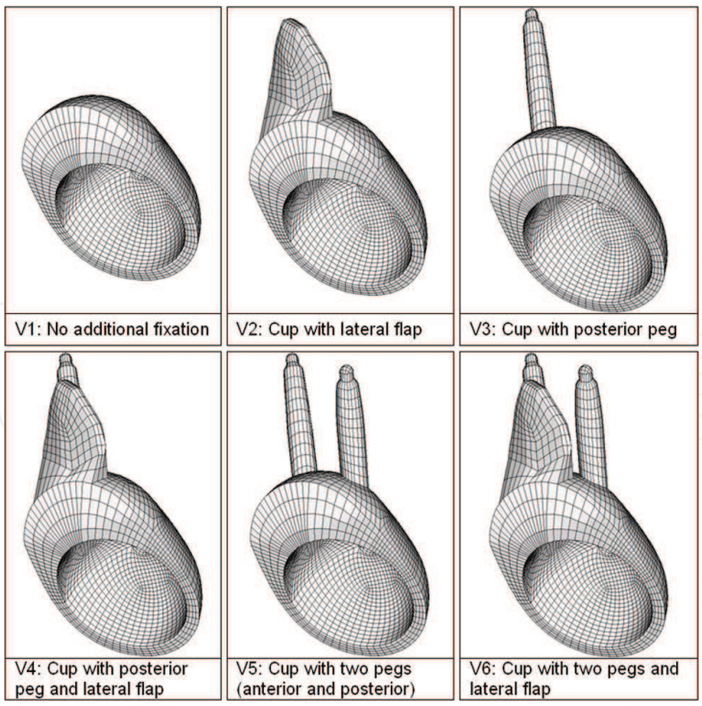

Fig. 10. Variations of the acetabular cup revision system concerning application of the lateral flap and the anterior end posterior fixation pegs. Each variant was virtually implanted into the hemipelvis and meshed with hexahedral elements.

In order to evaluate the influence of the fixation elements, six FE-models of the implant-bone-compound were generated with different variants of the modular acetabular cup revision system. Therefore, different combinations of the lateral flap and the anterior and posterior fixation pegs were virtually implanted, according to Fig. 10.
The structural response of the implant-bone compound to the applied forces was calculated nonlinearly using the solver Simulia/ABAQUS V 6.7 (Dassault Systèmes, RI, USA). The micromotion, being defined as the relative motion between implant and adjacent bone, was evaluated element-wise at the cup-bone interface.

3.3 Results

The micromotion of the cup revision system in the surrounding bone stock was evaluated using the relative tangential node displacements in the contact surface. The postprocessor ABAQUS enables the prediction of tangential displacements (CSLIP) in the two perpendicular directions t_1 und t_2 throughout the whole surface of the implant bed. The maximum amounts of micromotion u_{mic} were calculated in each finite element n by equation (4):

$$u_{mic}(n) = \sqrt{\left[CSLIP1(t_1, n)\right]^2 + \left[CSLIP2(t_2, n)\right]^2} \tag{4}$$

The results of the FE-analyses were plotted as a greyscale-figure for visualization. The micromotion under maximum loads during gait considering different combinations of fixation elements applied to the acetabular revision system are shown in Fig. 11.

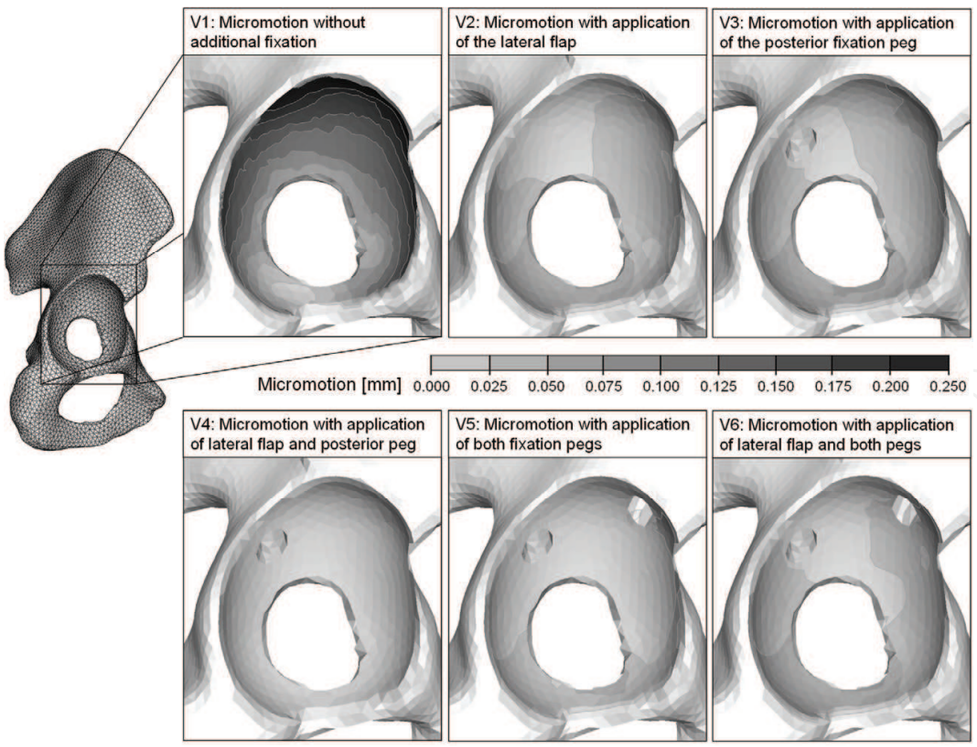

Fig. 11. Greyscale plot of the micromotion in the acetabular bone stock with a D'Antonio defect type III under the maximum loads and muscle forces during gait. Simulating the application of additional fixation elements, the micromotion was reduced significantly.

The interpretation of the results included firstly the maximum micromotion in the implant-bone interface, secondly the percentage of the contact surface with less than 50 µm micromotion.

The calculation of the revision cup without additional fixation (V1) showed high motion of the implant amounting up to 264 µm. Allowable micromotion of < 50 µm was found in the caudal acetabulum only within 5.7 % and 6.1 % of the whole contact surface during gait and during stair climbing. The application of the lateral flap (V2) resulted in a significant reduction of micromotion, especially in the cranial acetabulum. However, the caudal bone bed showed motion of up to 200 µm. Using the posterior fixation peg instead of the flap (V3) decreased the maximum micromotion to values below 100 µm. The areas of micromotion < 50 µm amounted 79 % of the whole contact area during gait and 84 % during stair climbing. When the posterior peg and the flap were used (V4), these areas increased up to 87 % and 98 %. The highest reduction of micromotion was reached using both fixation pegs (V5). In this case, the calculation showed no micromotion higher than 50 µm during gait and only 1 % of the contact area with micromotion higher than 50 µm during stair climbing. When the lateral flap was attached in addition to both pegs (V6), the amount of micromotion slightly increased.

Besides the evaluation of micromotion, the FE-analysis gives information about the expected stress states in the periprosthetic bone during load. Hence, bone regions with sparse amounts of stress which are subject to bone resorption can be identified. An adequate force transmission from the implant to the surrounding bone should enhance bone ongrowth as a result of reconstructed hip biomechanics. In the undesirable case of stress shielding, bone resorption could induce implant loosening. The present analysis was interpreted especially with regard to the bony region around the fixation pegs.

The greyscale plots in Fig. 12 show the stress states within the bone stock of the posterior fixation peg before and after implementation. The stress state without the peg clearly shows the cortical load transmission according to the sandwich-architecture of flat bones. If the fixation peg is inserted, the von-Mises stresses in the trabecular bone between the cortical walls increase up to 5.0 MPa. These stresses are an indicator for possible bone formation in the cranial part of the acetabulum as a result of stress-induced remodeling.

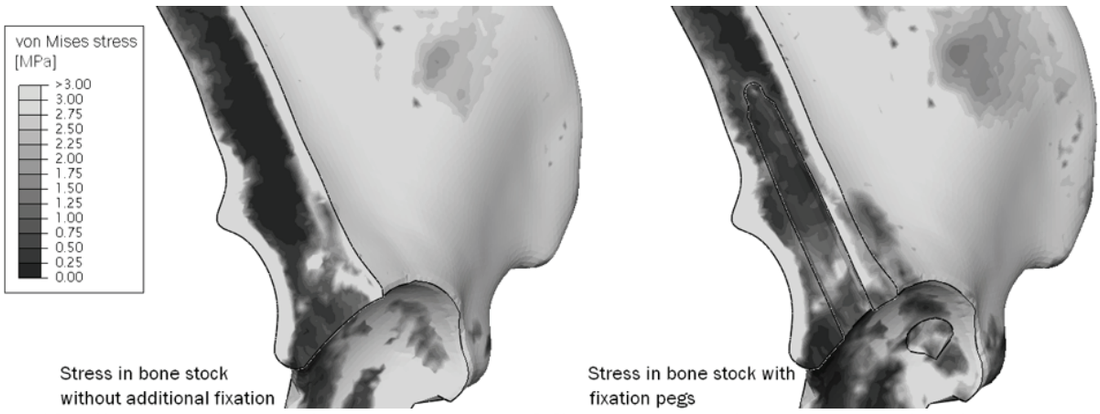

Fig. 12. Cross-sectional view of the von Mises stresses in the posterior ilium under maximum loads during gait. Stress plot with fixation pegs (right) shows higher internal stress in the trabecular bone than calculated without pegs (left).

4. Conclusion

Finite-element-analyses of the implant-bone-compound gained growing accuracy with the fast-paced development of computer workstations. There are a number of reasons why a biomechanical problem should be adressed and solved numerically using FEA:

1. The problem cannot be analyzed clinically:
    - Preclinical stage of implant development
    - Variation of a parameter which does not yet exist in implants on the market
    - Clinical study might not be sufficient to answer specific questions
    - Ethical reasons (e.g. dislocation modes of endoprostheses cannot be conducted in vivo)
2. The problem cannot be analyzed experimentally:
    - Analyzing many different parameters necessitates manufacturing of many prototypes and might be very cost-intensive
    - Boundary conditions such as muscle forces cannot be realized in an experimental setup
    - Experiments on human specimen may not be reproducible due to variations of biologic properties
3. Results from a clinical or experimental study cannot be interpreted
    - A numerical model can help interpreting clinical and experimental results

We presented an approach of how finite-element-models of the implant-bone-compound can be generated, and we gave an example of an FE-analysis of a new implant specifically designed to withstand loads and micromotion in large bone defects due to revision surgery. There is a variety of specifications made for modeling e.g. the pelvis in numerical analyses. The inhomogeneous material properties of trabecular bone as well as the varying thickness of the pelvic compacta should be considered (Anderson, Peters et al. 2005). For economic reasons, a hemipelvis can be modeled under symmetrical boundary conditions (Dalstra, Huiskes et al. 1995; Spears, Pfleiderer et al. 2001; Kaku, Tsumura et al. 2004; Oki, Ando et al. 2004; Anderson, Peters et al. 2005; Bachtar, Chen et al. 2006). The mapping of trabecular bone material data based on computed tomography scans is widely accepted (Dalstra, Huiskes et al. 1993; Dalstra, Huiskes et al. 1995; Anderson, Peters et al. 2005; Manley, Ong et al. 2006). Nevertheless, a dependency of compact bone stiffness and mineral content has not been proved yet.

Our approach to apply a temperature-dependent material model in combination with Hounsfield-Units treated mathematically as temperatures resulted in a good agreement of numerically and experimentally analyzed principal strains. The requirements for consideration of varying cortical thickness and inhomogeneous trabecular bone stiffness were satisfied. By assigning temperatures, the duration of the calculation was significantly decreased compared to assigning different Young's moduli to discrete trabecular volumes.

The finite-element-mesh of bone, if meshed with tetrahedral elements, should consist of tetrahedral elements with quadratic interpolation, i.e. at least 10 nodes per element. Besides the considerable increase in accuracy of such elements, the mapping of HU is realized on a higher node density.

It must be noted that development of finite-element-models in Orthopaedic Biomechanics goes far beyond the examples given in this article. Of course, different anatomical regions are being analyzed apart from the hip joint. There are numerous models of the knee joint,

spine, shoulder and many joints and bony regions in the human body (Fig. 13). Additionally, other disciplines close to orthopaedics deal with similar numerical approaches and models, e.g. traumatology and dental implantology.

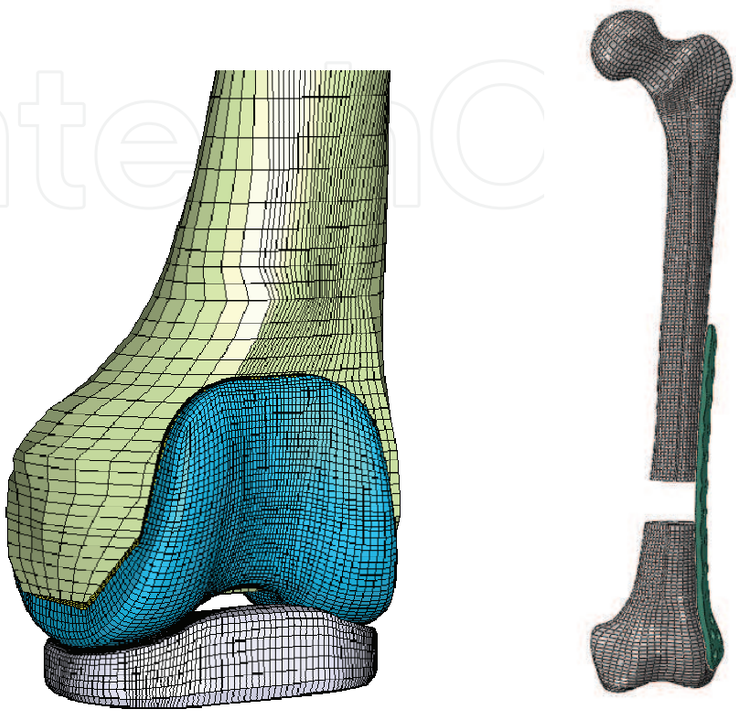

Fig. 13. Finite-element-models of a knee replacement with proximal femur (left) and an osteosyntheses with a segmental femoral bone defect (right)

But also the techniques in numerical simulation are varying. While the models presented in this section are all calculated statically, one also uses dynamic models for special questions. As an example, the impaction of implant components during surgery is in the focus of biomechanical modeling, thereby considering velocity-dependent damping forces as well as acceleration-dependent inertial forces.
Beyond that, more research groups concentrate on predicting biological effects in bone, e.g. the above mentioned bone remodeling initially described by Wolff's law.
In conclusion, finite-element-analysis yields a large potential to help in the development of sophisticated implants, surgery techniques and materials. But as depicted before (Fig. 1), a lively circle between clinical input and provision of analytical results conducted by the clinicians and the engineers is the basic requirement for fruitful research.

5. References

Aldinger, P. R., A. W. Jung, et al. (2005). Der zementfreie CLS-Titangeradschaft - Langzeitergebnisse, Indikationen und Limitationen. *Akt Traumatol* 35: 320-327.

Anderson, A. E., C. L. Peters, et al. (2005). Subject-specific finite element model of the pelvis: development, validation and sensitivity studies. *J Biomech Eng* 127(3): 364-73.

Bachtar, F., X. Chen, et al. (2006). Finite element contact analysis of the hip joint. *Med Biol Eng Comput* 44(8): 643-51.

Baker, R. (2003). ISB recommendation on definition of joint coordinate systems for the reporting of human joint motion-part I: ankle, hip and spine. *J Biomech* 36(2): 300-2; author reply 303-4.

Bergmann, G., G. Deuretzbacher, et al. (2001). Hip contact forces and gait patterns from routine activities. *J Biomech* 34(7): 859-71.

Bergmann, G., F. Graichen, et al. (1993). Hip joint loading during walking and running, measured in two patients. *J Biomech* 26(8): 969-90.

Chen, W. M., C. A. Engh, Jr., et al. (2000). Acetabular revision with use of a bilobed component inserted without cement in patients who have acetabular bone-stock deficiency. *J Bone Joint Surg AM* 82: 197.

Civinini, R., A. Capone, et al. (2007). Acetabular revisions using a cementless oblong cup: five to ten year results. *Int Orthop*.

D'Antonio, J. A., W. N. Capello, et al. (1989). Classification and management of acetabular abnormalities in total hip arthroplasty. *Clin Orthop Relat R* 420: 96-100.

D'Lima, D. D., S. Patil, et al. (2006). Tibial forces measured in vivo after total knee arthroplasty. *J Arthroplasty* 21(2): 255-62.

Dalstra, M., R. Huiskes, et al. (1993). Mechanical and textural properties of pelvic trabecular bone. *J Biomech* 26(4-5): 523-35.

Dalstra, M., R. Huiskes, et al. (1995). Development and validation of a three-dimensional finite element model of the pelvic bone. *J Biomech Eng* 117(3): 272-8.

Dearborn, J. T. and W. H. Harris (2000). Acetabular revision arthroplasty using so-called jumbo cementless components: an average 7-year follow-up study. *J Arthroplasty* 15: 8-15.

DeBoer, D. K. and M. J. Christie (1998). Reconstruction of the deficient acetabulum with an oblong prosthesis. *J Arthroplasty* 13(6): 674-680.

Gallo, J., Z. Rozkydal, et al. (2006). Reconstruction of severe acetabular bone defects using Burch-Schneider cage. *Acta Chir Orthop Traumatol Cech* 73(3): 157-63.

Garcia, J. M., M. Doblare, et al. (2000). Three-dimensional finite element analysis of several internal and external pelvis fixations. *J Biomech Eng* 122(5): 516-22.

Gerber, A., M. Pisan, et al. (2003). Ganz reinforcement ring for reconstruction of acetabular defects in revision total hip arthroplasty. *J Bone Joint Surg AM* 85(12): 2358-2364.

Götze, C., C. Sippel, et al. (2003). Grenzen der zementfreien Revisionsarthroplastik. *Z Orthop Grenzgeb* 141: 182-189.

Haury, J., F. Raeder, et al. (2004). Defekt-adaptiertes, modulares Revisions-Implantat bei Wechseloperationen. *Pressfitpfannen*. H. Effenberger, L. Zichner and J. Richolt. Grieskirchen, MCU**:** 221-226.

Heller, M. O., G. Bergmann, et al. (2001). Musculo-skeletal loading conditions at the hip during walking and stair climbing. *J Biomech* 34(7): 883-93.

Kaku, N., H. Tsumura, et al. (2004). Biomechanical study of load transfer of the pubic ramus due to pelvic inclination after hip joint surgery using a three-dimensional finite element model. *J Orthop Sci* 9(3): 264-9.

Keller, T. S. (1994). Predicting the compressive mechanical behavior of bone. *J Biomech* 27(9): 1159-68.

Kluess, D., R. Souffrant, et al. (2009). A convenient approach for finite-element-analyses of orthopaedic implants in bone contact: Modeling and experimental validation. *Comput Methods Programs Biomed* 95: 23-30.

Kurtz, S., F. Mowat, et al. (2005). Prevalence of primary and revision total hip and knee arthroplasty in the United States from 1990 through 2002. *J Bone Joint Surg Am* 87(7): 1487-97.

Malchau, H., P. Herberts, et al. (2002). The swedish total hip replacement register. *J Bone Joint Surg Am* 84-A Suppl 2: 2-20.

Manley, M. T., K. L. Ong, et al. (2006). The potential for bone loss in acetabular structures following THA. *Clin Orthop Relat Res* 453: 246-53.

Oki, H., M. Ando, et al. (2004). Relation between vertical orientation and stability of acetabular component in the dysplastic hip simulated by nonlinear three-dimensional finite element method. *Artif Organs* 28(11): 1050-4.

Perka, C. and R. Ludwig (2001). Reconstruction of segmental defects during revision procedures of the acetabulum with the Burch-Schneider anti-protrusio cage. *J Arthroplasty* 16: 568-574.

Perka, C., F. Schneider, et al. (2002). Revision acetabular arthroplasty using a pedestal cup in patients with previous congenital dislocation of the hip four case reports and review of treatment. *Arch Orthop Traum Su* 122: 237-240.

Peters, C. L., M. Curtain, et al. (1995). Acetabular revision with the Burch-Schneider antiprotrusio cage and cancellous allograft bone. *J Arthroplasty* 10: 307-312.

Rasmussen, J., M. Damsgaard, et al. (2003). Designing a general software system for musculoskeletal analysis. IX. International Symposium on Computer Simulation in Biomechanics, Sydney, Australia.

Rho, J. Y., M. C. Hobatho, et al. (1995). Relations of mechanical properties to density and CT numbers in human bone. *Med Eng Phys* 17(5): 347-55.

Schoellner, C. (2004). Die Sockelpfanne - eine Problemlösung für massive azetabuläre Pfannendefekte. *Pfannenrevisionseingriffe nach Hüft-TEP*. C. Perka and H. Zippel. Reinbek, Einhorn-Presse Verlag**:** 211-215.

Schultze, C., D. Kluess, et al. (2007). Finite element analysis of a cemented ceramic femoral component for the real assembly situation in total knee arthroplasty. *Biomed Tech (Berl)* 52(4): 301-7.

Siebenrock, K. A., A. Trochsler, et al. (2001). Die Hakendachschale in der Revision schwieriger gelockerter Hüftprothesenpfannen. *Orthopäde* 30: 273-279.

Snyder, S. M. and E. Schneider (1991). Estimation of mechanical properties of cortical bone by computed tomography. *J Orthop Res* 9(3): 422-31.

Spears, I. R., M. Pfleiderer, et al. (2001). The effect of interfacial parameters on cup-bone relative micromotions. A finite element investigation. *J Biomech* 34(1): 113-20.

Springer, B. D., T. K. Fehring, et al. (2009). Why revision total hip arthroplasty fails. *Clin Orthop Relat Res* 467(1): 166-173.

Thompson, M. S., M. D. Northmore-Ball, et al. (2002). Effects of acetabular resurfacing component material and fixation on the strain distribution in the pelvis. *Proc Inst Mech Eng [H]* 216(4): 237-45.

Wachtl, S. W., M. Jung, et al. (2000). The Burch-Schneider antiprotrusio cage in acetabular revision surgery: a mean follow-up of 12 years. *J Arthroplasty* 15: 959-963.

Weise, K. and E. Winter (2003). Revision arthroplasty--acetabular aspect: cementless acetabular bone reconstruction. *Int Orthop* 27: 29-36.

Whaley, A. L., D. J. Berry, et al. (2001). Extra-Large uncemented hemispherical acetabular components for revision total hip arthroplasty. *J Bone Joint Surg AM* 83: 1352-1357.

Wolff, J. (1892). *Das Gesetz der Transformation des Knochens*. Berlin, Hirschwald.

Wu, G., S. Siegler, et al. (2002). ISB recommendation on definitions of joint coordinate system of various joints for the reporting of human joint motion--part I: ankle, hip, and spine. International Society of Biomechanics. *J Biomech* 35(4): 543-8.

Wu, G., F. C. van der Helm, et al. (2005). ISB recommendation on definitions of joint coordinate systems of various joints for the reporting of human joint motion--Part II: shoulder, elbow, wrist and hand. *J Biomech* 38(5): 981-992.

Yoon, T. R., S. M. Rowe, et al. (2003). Acetabular revision using acetabular roof reinforcement ring with a hook. *J Arthroplasty* 18: 746-750.

Zacharias, T. (2001). *Präoperative biomechanische Berechnung von Femur-Hüftendoprothese-Systemen zur Ermittlung der individuellen Primärstabilität nach Roboterimplantation*. Aachen, Shaker Verlag.

Finite Element Analysis

Edited by David Moratal

ISBN 978-953-307-123-7

Hard cover, 688 pages

Publisher Sciyo

Published online 17, August, 2010

Published in print edition August, 2010

Finite element analysis is an engineering method for the numerical analysis of complex structures. This book provides a bird's eye view on this very broad matter through 27 original and innovative research studies exhibiting various investigation directions. Through its chapters the reader will have access to works related to Biomedical Engineering, Materials Engineering, Process Analysis and Civil Engineering. The text is addressed not only to researchers, but also to professional engineers, engineering lecturers and students seeking to gain a better understanding of where Finite Element Analysis stands today.

INTECH
open science | open minds

InTech Europe

University Campus STeP Ri
Slavka Krautzeka 83/A
51000 Rijeka, Croatia
Phone: +385 (51) 770 447
Fax: +385 (51) 686 166
www.intechopen.com

InTech China

Unit 405, Office Block, Hotel Equatorial Shanghai
No.65, Yan An Road (West), Shanghai, 200040, China
中国上海市延安西路65号上海国际贵都大饭店办公楼405单元
Phone: +86-21-62489820
Fax: +86-21-62489821

IntechOpen